

## DYNAMICAL MASSES FOR THE HYADES BINARY 80 TAURI

GUILLERMO TORRES

Center for Astrophysics | Harvard & Smithsonian, 60 Garden St., Cambridge, MA 02138, USA; gtorres@cfa.harvard.edu  
*Accepted for publication in The Astrophysical Journal*

### ABSTRACT

The empirical mass-luminosity relation in the Hyades cluster rests on dynamical mass determinations for five binary systems, of which one is eclipsing and the other four are visual or interferometric binaries. The last one was identified and first measured more than 20 years ago. Here we present dynamical mass measurements for a new binary system in the cluster, 80 Tau, which is also a visual system with a much longer orbital period of about 170 yr. Although we lack the radial-velocity information that has enabled the individual mass determinations in all of the previous binaries, we show that it is still possible to derive the component masses for 80 Tau using only astrometric observations. This is enabled by the accurate proper motion measurements from the *Hipparcos* and *Gaia* missions, which constrain the orbital acceleration in the plane of the sky. Separate proper motion values from *Gaia* for the primary and secondary provide a direct constraint on the mass ratio. Our mass measurements,  $M_A = 1.63^{+0.30}_{-0.13} M_\odot$  and  $M_B = 1.11^{+0.21}_{-0.14} M_\odot$ , are consistent with the mass-luminosity relation defined by the five previously known systems, which in turn is in good agreement with current models of stellar evolution.

### 1. INTRODUCTION

The empirical mass-luminosity relation (MLR) in the Hyades cluster has been the subject of numerous investigations over the past decades. This mapping between the mass of a star —its most fundamental property— and its brightness offers a valuable way to test models of stellar evolution in a homogeneous population with a well-known age (625 Myr; Perryman et al. 1998) and chemical composition ( $[\text{Fe}/\text{H}] = +0.18 \pm 0.03$ ; Dutra-Ferreira et al. 2016). Progress toward building the Hyades MLR has been relatively slow, however, as the essential ingredients are the dynamical masses, and only a handful of binary systems suitable for this type of determination have been found so far, and measured sufficiently well.

The first example was the 5.6-day eclipsing binary V818 Tau (HD 27130 = vB 22)<sup>1</sup>, discovered by McClure (1982), who published preliminary determinations of the individual masses that were subsequently refined by Schiller & Milone (1987). This remains the only known eclipsing binary in the cluster consisting of normal stars. Dynamical masses for a second system, the spectroscopic-interferometric binary  $\theta^2$  Tau (HD 28139 = vB 72,  $P = 141$  days), were reported by Peterson et al. (1993) and later revised by Tomkin et al. (1995) to remove an assumption on the mass ratio. Next came the long-period visual binaries 51 Tau (HD 27176 = vB 24,  $P = 11.3$  yr), 70 Tau (HD 27991 = vB 57,  $P = 6.3$  yr), and  $\theta^1$  Tau (HD 28307 = vB 71,  $P = 16.3$  yr), studied, respectively, by Torres et al. (1997a), Torres et al. (1997b), and Torres et al. (1997c). The primary of the latter binary is one of the four giants in the Hyades. All five systems have been revisited over the years by other authors with improvements in the dynamical masses in some cases, or in the absolute magnitudes, but no other binaries that are amenable to model-independent mass

determinations for the individual components have been found in more than 20 years.

In this paper we report the first dynamical mass measurements for a new system, 80 Tau (HD 28485 = vB 80 = ADS 3264), a bright ( $V = 5.55$ ),  $\sim 170$  yr visual binary discovered by Struve (1837). Its membership in the Hyades is well established (van Bueren 1952), and is supported by results from the *Gaia* mission, among many others. While the five previous systems have relied in part on spectroscopy (radial velocities) to infer the mass of each star, for 80 Tau this is not practical because of the long orbital period and the fact that the primary is a very rapid rotator ( $v \sin i \approx 180 \text{ km s}^{-1}$ ). This hinders the determination of velocities with the requisite precision. Nevertheless, as we show below, it is still possible to derive the individual masses using only astrometry. This is enabled by two types of complementary astrometric observations: *i*) ground-based measurements of the relative positions of the components collected by dozens of visual observers over a full cycle of the orbit; and *ii*) accurate parallaxes and proper motion (p.m.) measurements for both stars provided by the *Gaia* mission, and for the primary by *Hipparcos*. Together these p.m. constrain the mass ratio and contain valuable information on astrometric accelerations, by virtue of the 24-yr interval between the two space missions.

We describe the astrometric observations in Section 2. Our modeling of the orbital motion is discussed in Section 3, where we also present the results. We then use them in Section 4 to investigate the MLR in the Hyades and compare the empirical relation with current models of stellar evolution. Final remarks are given in Section 5.

### 2. ASTROMETRIC OBSERVATIONS

#### 2.1. Visual measurements

The discovery of 80 Tau as a visual binary is credited to Struve (1837), who first measured it in 1831 finding a companion some 2.5 magnitudes fainter at a distance of  $1''.74$  due north. In his honor the object also

<sup>1</sup> We provide for reference the vB designations originating with van Bueren (1952), which are also in common use in the literature.

carries the double star designation STF 554. Some 180 measurements of the position angle and angular separation ( $\theta$ ,  $\rho$ ) have been recorded in the 180 years since, the latest one in 2015. They cover a full orbital cycle, with a periastron passage around 1892. The vast majority of these observations were made with a classical filar micrometer, while a few of the more recent ones used the speckle interferometry technique or adaptive optics imaging. A listing of these measurements as contained in the Washington Double Star Catalog (WDS) was kindly provided by Brian Mason (U.S. Naval Observatory, Washington D.C.), with the dates of observation uniformly transformed from Besselian years to Julian years. To these we have added one observation from 1897 that was not included in the WDS listing, which was made by Burnham (1906) very close to periastron, and one from the *Gaia*/DR2 Catalogue (Gaia Collaboration et al. 2018) that we constructed by differencing the positions of the two components measured separately by the mission.

As a result of its long observational history, several visual orbits of 80 Tau have been computed over the years, and it was recognized early on as being a very eccentric and highly inclined system, such that all of the measurements are in the first quadrant. The orbit by Baize (1980), based on observations up to about 1975, is the one featured in the Sixth Catalog of Orbits of Visual Binary Stars<sup>2</sup> maintained at the U.S. Naval Observatory. According to Baize (1980) it has a period of 180 yr, a semimajor axis of  $1''00$ , an eccentricity of 0.82, and an inclination of  $107^\circ 6$ . However, that orbit no longer matches the more recent data. A revised model was proposed by Peterson & Solensky (1988) that is more eccentric ( $e = 0.901 \pm 0.027$ ), and a more recent one by Izmailov (2019) increases the eccentricity even further to  $0.979 \pm 0.011$ .

While a few of the recent visual observations of 80 Tau were published with corresponding uncertainties, most of them have no reported uncertainties at all. Because the quality of any particular measurement depends sensitively on many factors including the aperture used, the observing conditions, and even the experience and disposition of the observer, the task of assigning realistic uncertainties to observations of this kind is fraught with difficulty, and there is no unique way to do this. After some experimentation we have chosen to separate the observations into four groups, and to assign nominal uncertainties to the angular separations and position angles within each group. For the position angles the uncertainties were expressed in seconds of arc in the tangential direction,  $\sigma_t$ , to account explicitly for the dependence of the angular precision on angular separation:  $\sigma_t = \rho \sigma_\theta$ . This is important to properly weight the very few observations made near periastron, which were especially challenging for this binary given the telescopes in use at the time, as noted by Baize (1980). The four groups we considered are: 1) observations prior to 1900, which were all made with filar micrometers and small aperture telescopes; these were assigned errors of  $\sigma_\rho = 0''.13$  and  $\sigma_t = 0''.10$ ; 2) micrometer observations from 1900 to about 1975, which received  $\sigma_\rho$  and  $\sigma_t$  errors of  $0''.06$  and  $0''.025$ , respectively; 3) more recent micrometer measure-

ments ( $\sigma_\rho = 0''.03$  and  $\sigma_t = 0''.042$ ); and 4) speckle measurements without published uncertainties ( $\sigma_\rho = 0''.014$  and  $\sigma_t = 0''.012$ ). These values of  $\sigma_\rho$  and  $\sigma_t$  are the result of iterations of the analysis described later in Section 3 intended to achieve balanced residuals among the different groups, i.e., to establish the *relative weighting* among them. Further adjustments to the *absolute scale* of the separation and position angle errors are described below.

Two measurements of 80 Tau that were flagged as erroneous in the WDS were rejected, along with one position angle and three angular separation measurements that we found gave anomalously large residuals and were very different from others near in time. We also reversed the quadrant of an observation from 1886.97 that had previously been reversed in the WDS, as we found that the original angle as published fits our new orbit well. Finally, precession corrections were applied to all position angles to reduce them to the year 2000.0. In all we used 177 measures of the angular separation and 183 of the position angle. We list all observations in Table 1 along with their uncertainties and residuals from our adopted model orbit discussed below.

## 2.2. *Hipparcos* and *Gaia*

80 Tau is listed in both the *Hipparcos* Catalogue (HIP 20995; van Leeuwen 2007) and the *Gaia*/DR2 Catalogue (Gaia Collaboration et al. 2018), the latter containing separate entries for the primary and secondary.<sup>3</sup> The two *Gaia* estimates of the trigonometric parallax are consistent with each other, and with the *Hipparcos* value for the primary. Knowledge of the distance along with the visual orbit can then immediately provide a measure of the total mass of the system.

Beyond the visual observations described above, other constraints on the relative orbit that are available include the proper motions measured by the two missions, which are different. The mean epochs of those measurements are  $\sim 1991.25$  for *Hipparcos* and  $\sim 2015.5$  for *Gaia*. This 24-yr interval is long enough that orbital motion affects the p.m. determination at each epoch, providing a measure of the acceleration in the plane of the sky. Brandt (2018) performed a cross-calibration of the *Hipparcos* and *Gaia* catalogs to place them on the reference frame of *Gaia*/DR2, and produced a catalog of accelerations consisting of three nearly independent proper motions for each star: one p.m. near each mean epoch ( $\mu_H$  and  $\mu_G$  for *Hipparcos* and *Gaia*, with components in R.A. and Dec.), and a third measurement given by the *Gaia*-*Hipparcos* positional difference divided by the 24-yr time baseline ( $\mu_{HG}$ ). As this last quantity is usually much more precise than the other two, Brandt (2018) advocated subtracting  $\mu_{HG}$  from both  $\mu_H$  and  $\mu_G$ , which cancels out the motion of the barycenter (typically irrelevant for mass determinations). This gives two p.m. differences that are well suited for constraining the relative orbit of a binary (i.e., the total mass), even in cases where other types of observations cover only a fraction of the orbit. Examples of the use of this astrometric information combined with visual observations and with radial-velocity measurements to infer component masses for binaries were given by Dupuy et al. (2019) and Brandt et al. (2019).

<sup>2</sup> <https://ad.usno.navy.mil/wds/orb6.html>

<sup>3</sup> DR2 3312536927686011520 and DR2 3312536923393893120, respectively.

**Table 1**  
Visual Observations of 80 Tau

Year	$\theta$ (°)	$\sigma_t$ (")	$(O - C)_\theta$ (°)	$(O - C)_\theta/\sigma_\theta$	$\rho$ (")	$\sigma_\rho$ (")	$(O - C)_\rho$ (")	$(O - C)_\rho/\sigma_\rho$
1831.18	12.9	0.146	-3.68	-0.71	1.74	0.193	0.139	0.72
1836.96	9.8	0.146	-6.14	-1.15	1.5	0.193	-0.059	-0.30
1837.22	11.0	0.146	-4.91	-0.92	1.4	0.193	-0.156	-0.81
1839.16	13.9	0.146	-1.79	-0.33	1.6	0.193	0.061	0.31
1840.12	14.8	0.146	-0.78	-0.14	1.66	0.193	0.130	0.67

**Note.** — The position angles listed are the original ones; precession corrections were applied internally during the orbital analysis. The uncertainties listed in the table correspond to the  $\sigma_\rho$  and  $\sigma_t$  values given in the text multiplied by the scaling factors  $f_\rho$  and  $f_\theta$  reported in Section 3, and represent the final errors used in the solution described there. We also list the residuals in angular separation and position angle normalized to their uncertainties  $\sigma_\rho$  and  $\sigma_\theta = \sigma_t/\rho$ . (This table is available in its entirety in machine-readable form.)

In those studies the radial velocities (typically in the form of a measured velocity change for the primary) served to provide the necessary constraint on the mass ratio, which then enabled the individual masses to be calculated. For 80 Tau we unfortunately lack sufficiently precise measurements of the radial velocities of the components to show a statistically significant change with time. This is due to the fact that the orbital period is very long and we happen to be far from periastron, so that the stars are now moving very slowly at about the same speed when projected along the line of sight, i.e., the spectral lines are completely blended. Furthermore, the primary star is a rapid rotator ( $v \sin i = 180 \text{ km s}^{-1}$ ; Royer et al. 2002), making precise velocity measurements extraordinarily difficult.<sup>4</sup> Thus, we are missing the spectroscopic constraint on the mass ratio.

However, because *Gaia* measured the proper motion of both components ( $\mu_{G,A}$ ,  $\mu_{G,B}$ ), and the values are appreciably different, there is astrometric information on the mass ratio that comes from the fact that the orbits of the two stars around their common center of mass perturb the p.m. measured by *Gaia* in different ways that are directly related to their masses. Conceptually, then, provided the p.m. of the center of mass ( $\mu_0$ ) can be determined, the ratio between the differences  $\mu_{G,A} - \mu_0$  and  $\mu_{G,B} - \mu_0$  yields the mass ratio  $M_B/M_A$ . This is analogous to the situation in the direction perpendicular to the plane of the sky, in which a single measurement of the primary and secondary radial velocity in a binary at a given time is sufficient to establish the mass ratio if the center-of-mass velocity is known. The accuracy of the mass ratio determination from the proper motions will depend critically on how well the motion of the barycenter can be constrained by other measurements.

To implement this idea we therefore proceeded differently than advocated by Brandt (2018): instead of using the differences  $\mu_H - \mu_{HG}$  and  $\mu_G - \mu_{HG}$  for the primary as our measurements to supplement the constraint on the relative orbit provided by the visual observations, we used the four p.m. measurements  $\mu_H$ ,  $\mu_{HG}$ ,  $\mu_{G,A}$  and  $\mu_{G,B}$  as independent observables to constrain the orbits

<sup>4</sup> The many existing velocity measurements of this bright star in the literature show considerable scatter most likely due to this difficulty (Abt et al. 1980). A claim has been made of periodic variability with an orbital period of 30.5 days and a center-of-mass velocity of  $\gamma = +29.3 \text{ km s}^{-1}$  (Heintz 1981). This seems dubious, however, as  $\gamma$  is more than  $10 \text{ km s}^{-1}$  lower than the velocity expected for 80 Tau from its position in the cluster, and especially since more recent velocity measurements have failed to follow that orbit.

of both stars (and therefore their mass ratio), and to solve for  $\mu_0$  at the same time. These four measurements are listed in Table 2 along with the correlation coefficients between the R.A. and Dec. components as given by Brandt (2018) or the *Gaia* Catalogue. We also give the mean epoch in each coordinate, as well as the parallaxes. The *Hipparcos* parallax we report is the result of combining the values from the revised and original versions of the catalog (ESA 1997; van Leeuwen 2007) in the same 60/40 proportions as recommended by Brandt (2018), adding the same 0.20 mas error inflation in quadrature as prescribed by his Eq.(18). The uncertainty for the *Gaia* p.m. of the secondary has also been adjusted upward as prescribed by Brandt (2018).

### 3. ANALYSIS AND RESULTS

Our procedure combines the visual observations with the four p.m. measurements from *Hipparcos* and *Gaia* into a single solution. The visual orbit is described by the orbital period ( $P$ ), the semimajor axis ( $a$ ), the eccentricity parameters  $\sqrt{e} \cos \omega_B$  and  $\sqrt{e} \sin \omega_B$  (where  $e$  is the eccentricity and  $\omega_B$  the longitude of periastron for the secondary), the cosine of the orbital inclination angle ( $\cos i$ ), the position angle of the ascending node<sup>5</sup> for the equinox J2000 ( $\Omega$ ), and a reference time of periastron passage ( $T$ ). Additionally we solved for the mass fraction  $f = M_B/(M_A + M_B)$  (more convenient for our purposes than the mass ratio) and the R.A. and Dec. components of the proper motion of the barycenter,  $\mu_{\alpha,0}^*$  and  $\mu_{\delta,0}$ . The notation  $\mu_{\alpha}^*$  we use here and in the following represents the p.m. in R.A. multiplied by the cosine of the Declination.

Our method of solution used the `emcee`<sup>6</sup> code of Foreman-Mackey et al. (2013), which is a Python implementation of the affine-invariant Markov Chain Monte Carlo (MCMC) ensemble sampler proposed by Goodman & Weare (2010). We used 100 walkers with 20,000 links each, after discarding the burn-in, and priors for all variables were assumed to be uniform except for  $P$  and  $a$ , for which we used log-uniform priors. To establish the optimal relative weighting between the angular separation and position angle measurements we included two more parameters,  $f_\rho$  and  $f_\theta$ , which represent multiplicative scaling factors for the uncertainties described in Section 2.1. They are intended to result in reduced

<sup>5</sup> In the absence of radial velocity information we followed the usual convention of assuming the node for which  $\Omega < 180^\circ$  to be the ascending node.

<sup>6</sup> <https://emcee.readthedocs.io/en/v2.2.1/>

**Table 2**  
Proper Motion and Parallax Information for 80 Tau from *Gaia*/DR2 and *Hipparcos*

Source	Comp	$\mu_\alpha^*$ (mas yr <sup>-1</sup> )	$\mu_\delta$ (mas yr <sup>-1</sup> )	Corr	Average Epoch	$\pi$ (mas)
HIP	A	+107.33 ± 1.05	-23.56 ± 0.64	-0.090	1991.35 / 1991.04	22.26 ± 1.01
<i>Gaia</i> -HIP	A	+108.446 ± 0.034	-23.719 ± 0.021	+0.244	...	...
<i>Gaia</i>	A	+108.92 ± 0.43	-22.14 ± 0.27	-0.293	2015.58 / 2015.63	21.12 ± 0.12
<i>Gaia</i>	B	+102.57 ± 0.30	-31.43 ± 0.15	-0.314	2015.58 / 2015.63	20.934 ± 0.069

**Note.** — The first three entries are taken from the acceleration catalog of Brandt (2018); the last is from *Gaia*/DR2. “Comp” refers to the primary or secondary component,  $\mu_\alpha^*$  represents the p.m. in R.A. multiplied by the cosine of the Declination, and “Corr” is the correlation coefficient between the proper motions in R.A. and Dec. The “Average Epoch” is given separately for the p.m. measurements in R.A. and Dec. The *Hipparcos* parallax was calculated from the values reported in the revised and original versions of the catalog (ESA 1997; van Leeuwen 2007) with the same 60/40 linear combination recommended by Brandt (2018), following his Eq.(18).

$\chi^2$  values near unity for each type of observation, and were solved for simultaneously and self-consistently with the other parameters (see Gregory 2005). The adopted priors for  $f_\rho$  and  $f_\theta$  were log-uniform. Convergence of our MCMC procedure was checked by visual inspection of the chains, and by requiring a Gelman-Rubin statistic (Gelman & Rubin 1992) less than 1.05 for all 12 adjustable parameters. Our likelihood function is

$$\ln \mathcal{L} = -0.5(\chi_\rho^2 + \chi_\theta^2 + \chi_H^2 + \chi_{HG}^2 + \chi_{G,A}^2 + \chi_{G,B}^2),$$

where the chi-squared terms in this expression are

$$\begin{aligned} \chi_\rho^2 &= \sum_{i=1}^{N_\rho} \frac{(\rho_i - \hat{\rho}[t_i])^2}{(f_\rho \sigma_\rho)^2} + \sum_{i=1}^{N_\rho} \ln(f_\rho \sigma_\rho)^2 \\ \chi_\theta^2 &= \sum_{i=1}^{N_\theta} \frac{(\theta_i - \hat{\theta}[t_i])^2}{(f_\theta \sigma_\theta)^2} + \sum_{i=1}^{N_\theta} \ln(f_\theta \sigma_\theta)^2 \\ \chi_H^2 &= (\mu_{\alpha,H}^* - \hat{\mu}_{\alpha,H}^*)^2 C_{\alpha\alpha,H}^{-1} + (\mu_{\delta,H} - \hat{\mu}_{\delta,H})^2 C_{\delta\delta,H}^{-1} \\ &\quad + 2(\mu_{\alpha,H}^* - \hat{\mu}_{\alpha,H}^*)(\mu_{\delta,H} - \hat{\mu}_{\delta,H}) C_{\alpha\delta,H}^{-1} \\ \chi_{HG}^2 &= (\mu_{\alpha,HG}^* - \hat{\mu}_{\alpha,HG}^*)^2 C_{\alpha\alpha,HG}^{-1} \\ &\quad + (\mu_{\delta,HG} - \hat{\mu}_{\delta,HG})^2 C_{\delta\delta,HG}^{-1} \\ &\quad + 2(\mu_{\alpha,HG}^* - \hat{\mu}_{\alpha,HG}^*)(\mu_{\delta,HG} - \hat{\mu}_{\delta,HG}) C_{\alpha\delta,HG}^{-1} \\ \chi_{G,A}^2 &= (\mu_{\alpha,G,A}^* - \hat{\mu}_{\alpha,G,A}^*)^2 C_{\alpha\alpha,G,A}^{-1} \\ &\quad + (\mu_{\delta,G,A} - \hat{\mu}_{\delta,G,A})^2 C_{\delta\delta,G,A}^{-1} \\ &\quad + 2(\mu_{\alpha,G,A}^* - \hat{\mu}_{\alpha,G,A}^*)(\mu_{\delta,G,A} - \hat{\mu}_{\delta,G,A}) C_{\alpha\delta,G,A}^{-1} \\ \chi_{G,B}^2 &= (\mu_{\alpha,G,B}^* - \hat{\mu}_{\alpha,G,B}^*)^2 C_{\alpha\alpha,G,B}^{-1} \\ &\quad + (\mu_{\delta,G,B} - \hat{\mu}_{\delta,G,B})^2 C_{\delta\delta,G,B}^{-1} \\ &\quad + 2(\mu_{\alpha,G,B}^* - \hat{\mu}_{\alpha,G,B}^*)(\mu_{\delta,G,B} - \hat{\mu}_{\delta,G,B}) C_{\alpha\delta,G,B}^{-1}, \end{aligned}$$

in which the proper motions from *Hipparcos* correspond to the primary. The  $C^{-1}$  terms are the relevant elements of the inverse of the covariance matrix, which we computed from the uncertainties and correlations given in Table 2.

The model-predicted quantities  $\hat{\rho}$  and  $\hat{\theta}$  in the expressions above are a function of the elements of the relative orbit. The quantities  $\hat{\mu}_{\alpha,H}^*$ ,  $\hat{\mu}_{\alpha,G,A}^*$ , and  $\hat{\mu}_{\alpha,G,B}^*$ , and similar ones for the Declination components, were computed by adding a perturbation to the p.m. of the barycenter calculated from the temporal change in the position in the orbit of the relevant star. For example,

$\hat{\mu}_{\alpha,G,A}^* = \mu_{\alpha,0}^* + \Delta\mu_{\alpha,G,A}^*$ , in which the last term is the derivative of the orbital position of the primary relative to the barycenter at the time of the *Gaia* measurement as listed in Table 2. Even though *Hipparcos* and *Gaia* observed 80 Tau during a finite period of time (about 2.5 and 1.7 years, respectively), those intervals are much shorter than the orbital period, so we have considered the proper motions to be effectively instantaneous.

In a similar fashion, we computed  $\hat{\mu}_{\alpha,HG}^*$  as

$$\hat{\mu}_{\alpha,HG}^* = \mu_{\alpha,0}^* + \frac{\Delta\alpha_{G,A}^*[t_{\alpha,G}] - \Delta\alpha_H^*[t_{\alpha,H}]}{t_{\alpha,G} - t_{\alpha,H}},$$

in which the  $\Delta\alpha^*$  quantities represent the position of the primary relative to the barycenter at the mean epoch of each catalog, and are easily calculated from the orbital elements. A similar equation was used for  $\hat{\mu}_{\delta,HG}$ .

The MCMC solutions were repeated several times to manually fine-tune the uncertainties  $\sigma_\rho$  and  $\sigma_t$  that we assigned to each of the four groups into which we separated the visual observations (Section 2.1). This was done to set the relative weighting among groups. During each of those solutions we simultaneously allowed the model to freely adjust the  $f_\rho$  and  $f_\theta$  factors in order to balance the relative weight of the angular separation and position angle measurements by setting the absolute scale of their errors. This process led to the final  $\sigma_\rho$  and  $\sigma_t$  values given earlier in Section 2.1.

The results of our analysis are presented in Table 3, with an indication of the priors used for each adjustable parameter. The bottom section of the table gives the derived quantities computed directly from the chains of adjusted elements, including the masses, the linear semi-major axis, and periastron distance  $a(1-e)$ . The scaling needed to compute these derived quantities is set by the parallax, which we assumed to be uncorrelated with the other properties, and which is given by the weighted average of the values in Table 2. We list this average parallax in the table as well. In each case we report the mode of the posterior distributions, along with the 68.3% credible intervals. Table 4 lists the correlation coefficients among all adjustable parameters, with the highest ones underlined.

The eccentricity,  $e = 0.915_{-0.018}^{+0.020}$ , is found to be less extreme than the latest reported value of  $0.979 \pm 0.011$  by Izmailov (2019).<sup>7</sup> Our semimajor axis is some-

<sup>7</sup> We note that the study of Izmailov (2019) reported two orbital solutions for 80 Tau: one in which all observations were given equal

**Table 3**  
Results of our MCMC Analysis for 80 Tau

Parameter	Value	Prior
$P$ (year)	$172.5^{+2.0}_{-2.1}$	[2, 7]
$a$ (arcsec)	$0.908^{+0.044}_{-0.017}$	[-2, 2]
$\sqrt{e} \cos \omega_B$	$-0.897^{+0.058}_{-0.025}$	[-1, 1]
$\sqrt{e} \sin \omega_B$	$0.34^{+0.13}_{-0.11}$	[-1, 1]
$\cos i$	$-0.432^{+0.035}_{-0.058}$	[-1, 1]
$\Omega_{2000}$ (degree)	$10.8^{+2.7}_{-4.7}$	[-180, 180]
$T$ (year)	$1891.9^{+1.5}_{-1.7}$	[1800, 2000]
$f \equiv M_B / (M_A + M_B)$	$0.402^{+0.040}_{-0.043}$	[0, 1]
$\mu_{\alpha,0}^*$ (mas yr $^{-1}$ )	$+106.41^{+0.23}_{-0.23}$	[80, 120]
$\mu_{\delta,0}$ (mas yr $^{-1}$ )	$-25.72^{+0.25}_{-0.27}$	[-50, 0]
$f_\rho$	$1.487^{+0.087}_{-0.074}$	[-5, 3]
$f_\theta$	$1.454^{+0.083}_{-0.071}$	[-5, 3]
Derived quantities		
$e$	$0.915^{+0.020}_{-0.018}$	...
$\omega_B$ (degree)	$159.2^{+6.4}_{-8.6}$	...
$i$ (degree)	$115.5^{+3.8}_{-2.1}$	...
$M_A + M_B$ ( $M_\odot$ )	$2.72^{+0.46}_{-0.17}$	...
$M_A$ ( $M_\odot$ )	$1.63^{+0.30}_{-0.13}$	...
$M_B$ ( $M_\odot$ )	$1.11^{+0.21}_{-0.14}$	...
$q \equiv M_B / M_A$	$0.66^{+0.13}_{-0.10}$	...
$\pi$ (mas)	$20.984^{+0.060}_{-0.060}$	...
Distance (pc)	$47.66^{+0.14}_{-0.14}$	...
$a$ (au)	$43.26^{+2.09}_{-0.80}$	...
$a(1 - e)$ (au)	$3.67^{+0.78}_{-0.79}$	...

**Note.** — The values listed correspond to the mode of the respective posterior distributions, and the uncertainties represent the 68.3% credible intervals. All priors are uniform over the specified ranges, except for  $P$ ,  $a$ ,  $f_\rho$  and  $f_\theta$ , which are log-uniform. The parallax reported is the weighted average of the values listed in Table 2.

weight, and another in which the measurements were weighted differently. Both were computed using a least-squares method followed by a Monte Carlo sampling experiment to infer uncertainties. The adopted weights for the second solution resulted from a complicated procedure that is not entirely clear to the present author, apparently involving an assessment of measurement residuals from different sources and also from other binaries, although no specific details were given for 80 Tau. The solution favored by Izmailov (2019) is the one that uses different weights, which gives the eccentricity we reported. In the other solution the eccentricity is slightly smaller ( $e = 0.925 \pm 0.019$ ). However, it is puzzling to see that the weighted solution has considerably larger uncertainties for most of the elements than the unweighted one, some of which are surprisingly large. The angular semimajor axis, for example, was reported as  $a = 1''.03 \pm 0''.48$ , whereas the corresponding result from the unweighted orbit is  $1''.02 \pm 0''.08$ . Similarly with the orientation angles, which have uncertainties of tens of degrees in the weighted model, versus single digits for the unweighted one. As a result, the implied total mass of the binary from the weighted solution (adopting the parallax in Table 3) is  $4.0 \pm 8.4 M_\odot$ , which is not only of little use but is also much worse than the value from the unweighted solution,  $4.0 \pm 1.0 M_\odot$ .

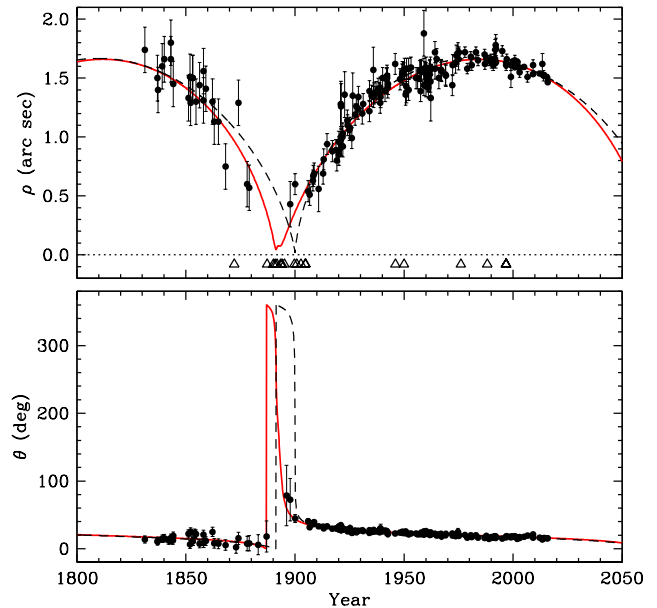


**Figure 1.** Observations of 80 Tau along with our adopted model from Table 3. The dashed line represents the orbit by Izmailov (2019). Also shown in the top panel are the dates of the observations that did not resolve the binary (triangles).

what smaller compared to the estimates by both Baize (1980) and Izmailov (2019), but larger than that of Peterson & Solensky (1988). Our adopted model is shown in Figure 1 along with the observations, with the orbit by Izmailov (2019) added for reference (see footnote 7). We find that our orbit and that of Izmailov (2019) provide an equally good fit to the observations after periastron, but that ours represents the earlier measurements slightly better. Observations for which the observers reported the binary to be unresolved are marked in the top panel of Figure 1 with triangles; they are seen to be mostly at periastron, though a few have occurred at other times reflecting the difficulty of detecting the faint secondary, or perhaps poor observing conditions. A rendering of the orbit in polar coordinates is seen in Figure 2. The predicted radial-velocity difference between the components at the present time is only  $2.1 \text{ km s}^{-1}$ , and will increase very slowly to about  $2.2 \text{ km s}^{-1}$  by the year 2025 and  $2.3 \text{ km s}^{-1}$  by 2030.

#### 4. THE MASS-LUMINOSITY RELATION IN THE HYADES

Separate brightness measurements for the components of the 80 Tau binary are available from the Tycho-2 Catalogue (Høg et al. 2000). Conversion of those  $B_T$  and  $V_T$  magnitudes to the Johnson system gives  $V$ -band magnitudes of  $5.674 \pm 0.010$  and  $8.055 \pm 0.016$ . Absolute visual magnitudes then follow from the distance to the system (Table 3), and are  $M_V^A = 2.283 \pm 0.012$  and  $M_V^B = 4.664 \pm 0.017$ , ignoring extinction. Although brightness measurements for both components are also given in the *Gaia*/DR2 catalog, the values for the secondary star in the blue and red bandpasses ( $G_{BP}$  and  $G_{RP}$ ) are very uncertain and potentially biased, according to the accompanying quality flag, and we do not use them here. Conversion of the flux measurements for the primary to the Johnson system using the relation by Evans et al. (2018) gives a value consistent with the one above ( $V = 5.641 \pm 0.046$ ).

**Table 4**  
Correlation Coefficients Among the Adjusted Parameters of 80 Tau

$\ln P$	+1.000	...	...	...	...	...	...	...	...	...	...	...
$\ln a$	-0.420	+1.000	...	...	...	...	...	...	...	...	...	...
$\sqrt{e} \cos \omega_B$	-0.504	<u>+0.984</u>	+1.000	...	...	...	...	...	...	...	...	...
$\sqrt{e} \sin \omega_B$	-0.639	<u>+0.906</u>	<u>+0.952</u>	+1.000	...	...	...	...	...	...	...	...
$\cos i$	+0.498	<u>+0.307</u>	<u>+0.168</u>	+0.001	+1.000	...	...	...	...	...	...	...
$\Omega_{2000}$	+0.742	-0.788	-0.876	<u>-0.948</u>	+0.289	+1.000	...	...	...	...	...	...
$T$	-0.316	-0.631	-0.547	<u>-0.451</u>	-0.747	+0.193	+1.000	...	...	...	...	...
$f$	-0.158	+0.038	-0.016	-0.032	+0.195	+0.095	-0.072	+1.000	...	...	...	...
$\mu_{\alpha,0}^*$	+0.151	+0.004	+0.053	+0.067	-0.132	-0.110	+0.035	<u>-0.978</u>	+1.000	...	...	...
$\mu_{\delta,0}$	+0.143	+0.049	+0.104	+0.119	-0.171	-0.170	+0.005	<u>-0.981</u>	<u>+0.971</u>	+1.000	...	...
$\ln f_\rho$	+0.051	+0.013	+0.008	-0.027	+0.055	+0.034	-0.010	<u>-0.028</u>	<u>+0.033</u>	+0.032	+1.000	...
$\ln f_\theta$	-0.065	+0.040	+0.043	+0.051	-0.061	-0.064	+0.013	+0.012	-0.016	-0.013	-0.019	+1.000
	$\ln P$	$\ln a$	$\sqrt{e} \cos \omega_B$	$\sqrt{e} \sin \omega_B$	$\cos i$	$\Omega_{2000}$	$T$	$f$	$\mu_{\alpha,0}^*$	$\mu_{\delta,0}$	$\ln f_\rho$	$\ln f_\theta$

**Note.** — Correlation coefficients larger than 0.900 in absolute value are underlined.

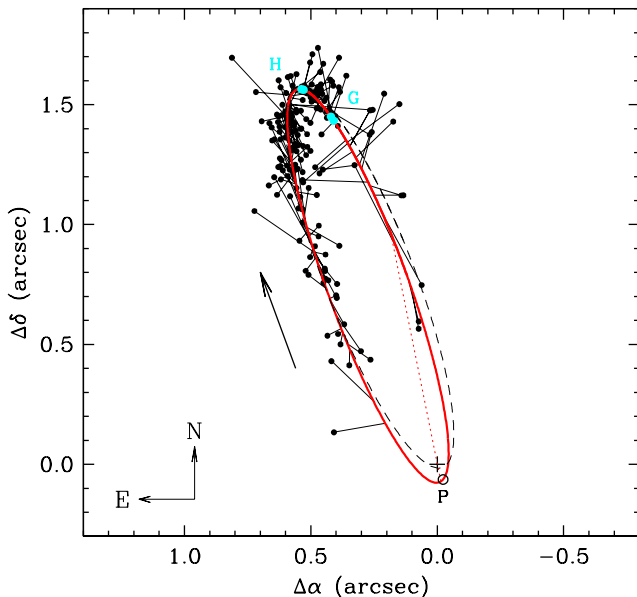


**Figure 2.** Same as Figure 1 in polar coordinates, again showing the orbit by Izmailov (2019) with a dashed line, for reference. The direction of motion (retrograde) is indicated by the arrow. Thin lines connect each observation with the predicted position in the orbit. The plus sign marks the position of the primary, and the dotted line is the line of nodes. Periastron is indicated with an open circle at the bottom, labeled “P”. The epochs of the *Hipparcos* and *Gaia* observations (1991.25 and 2015.5) are indicated with larger cyan filled circles near the top.

These absolute magnitudes and our dynamical masses offer a valuable opportunity to revisit the empirical MLR in the Hyades, especially given that mass estimates (and in some cases the absolute magnitudes) for some of the previously known systems have been revised in recent years. A summary of those revisions is presented below.

•  **$\theta^2$  Tau.** The dynamical masses by Tomkin et al. (1995) were improved by Torres et al. (1997c), and were supplemented with absolute magnitudes derived from the orbital parallax. Armstrong et al. (2006) made use of new interferometric observations and the mass ratio from the previous study, and revised the masses downward by about  $0.25 M_\odot$ , also making the uncertainties somewhat smaller. They replaced the orbital parallax of the system with a dynamical parallax, but obtained very nearly the same absolute magnitudes. Subsequently Lampens et al. (2009) reported new spectroscopic results from spectral

disentangling that improved the mass uncertainties by a factor of several, but made both masses larger again. In the case of the primary ( $2.58 \pm 0.04 M_\odot$ ), which is a well known  $\delta$  Sct star, the result is formally larger than the expected turnoff mass of the cluster ( $\sim 2.4 M_\odot$ ). This is difficult to understand. A more recent disentangling study by Torres et al. (2011)<sup>8</sup> also resulted in small errors, and an even larger primary mass ( $2.86 \pm 0.06 M_\odot$ ) that seems implausible for a main-sequence star in the Hyades (see also the remarks by Brandt & Huang 2015). It is unclear what may be causing these larger masses from the spectral disentangling technique. Consequently, and until those results can be understood, the determinations by Armstrong et al. (2006) seem preferable.

• **51 Tau.** The original mass determinations by Torres et al. (1997a) were revised by Martin et al. (1998) using the *Hipparcos* astrometry combined with a relative astrometric orbit from Balega & Balega (1988), which resulted in a lower mass sum, a lower mass ratio, but significantly larger uncertainties. Söderhjelm (1999) also combined *Hipparcos* observations with ground-based data, reporting masses closer to those from the original determination though again with larger uncertainties. The details of his solution were not given. We have chosen to accept the Torres et al. (1997a) results.

• **70 Tau.** The only published dynamical mass determinations for this binary are those of Torres et al. (1997b), which we adopt.

•  **$\theta^1$  Tau.** The original mass determinations by Torres et al. (1997c) were revised by Lebreton et al. (2001) using the relative orbit from the previous study and a slightly larger dynamical parallax than that employed earlier. The mass values are not very different, but the uncertainties for the primary mass and for the absolute magnitudes are slightly smaller, so we selected those results.

• **V818 Tau.** The mass determinations of Schiller & Milone (1987) were slightly updated by Peterson & Solensky (1988). The latest estimates of the masses and absolute visual magnitudes of this eclipsing system are those of Torres & Ribas (2002), which we use in the following. The precision of the primary mass is slightly improved.

The adopted values for these five binaries (excluding

<sup>8</sup> No relation to the present author.

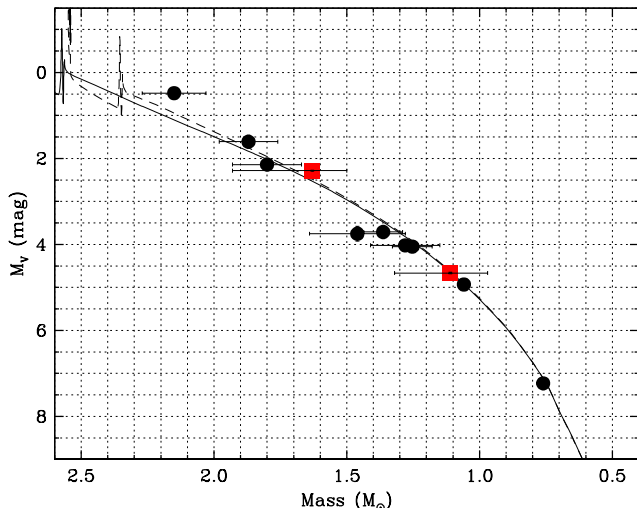


**Figure 3.** Empirical mass-luminosity relation in the Hyades based on the six binary systems in the cluster with dynamical mass determinations for the individual components (Table 5). Square symbols represent the estimates for 80 Tau from this work. Isochrones from the PARSEC series (Chen et al. 2014) are shown for ages of 625 Myr (solid line) and 800 Myr (dashed), for a fixed cluster metallicity of  $[\text{Fe}/\text{H}] = +0.18$ .

the giant primary of  $\theta^1$  Tau) are collected in Table 5 in order of decreasing primary mass. Our own determinations for 80 Tau are added for completeness. To our knowledge these are the only binary systems in the Hyades with dynamical mass determinations for the individual components. While several other systems in the cluster have known visual orbits, they can only provide a total mass (when combined, e.g., with parallaxes from *Gaia*), and are therefore not useful for our purpose.

#### 4.1. Comparison with Models

The empirical mass-luminosity relation based on the data in Table 5 is presented in Figure 3. Measurements for 80 Tau are represented with square symbols. Stellar evolution models from the PARSEC series by Chen et al. (2014) corresponding to a metallicity of  $[\text{Fe}/\text{H}] = +0.18$  are shown as well, for ages of 625 Myr (e.g., Perryman et al. 1998) and also 800 Myr (Brandt & Huang 2015). Other model isochrones such as those from the MIST series (Choi et al. 2016) are almost indistinguishable in this diagram, and are not shown. The agreement between theory and observation is quite satisfactory, with nearly all mass estimates being consistent with the isochrones within the (admittedly large) observational errors, some of which exceed 10%. The highly asymmetric error bars for the masses of 80 Tau are a consequence of the shape of the posterior distributions.

While our choices above regarding the sources for the dynamical masses of the five previously studied binaries have generally been driven by the level of precision (formal errors), this is not necessarily a guarantee of accuracy. We note, for example, that adopting the masses of Söderhjelm (1999) for 51 Tau instead of those of Torres et al. (1997a) would give a virtually perfect match to the models, though with larger error bars. Similarly, the more uncertain masses of Torres et al. (1997c) for  $\theta^2$  Tau agree better with theory than those of Armstrong et al. (2006). Both of these may well be

accidental agreements. In any case, an underlying weakness of many if not all of the Hyades mass determinations is the fact that they have often used partial results from earlier studies such as fixed visual orbital elements, fixed velocity semi-amplitudes, fixed mass ratios, etc., rather than the original data on which those external constraints were based. This is not optimal. In some cases this was done because the original data were not available. Although it is beyond the scope of the present study, a reanalysis of several of these systems would be beneficial, and could improve not only the precision but also the accuracy of the mass determinations. For some of the binaries more than 20 years have passed since the last detailed analysis (which is longer than a full orbital cycle even for  $\theta^1$  Tau, with  $P = 16.3$  yr), and new and better observations may be available.

#### 5. CONCLUDING REMARKS

We have measured the absolute masses of the components of the Hyades visual binary 80 Tau, only the sixth system with individual dynamical mass determinations in the cluster, and the first to be identified in more than 20 years. It is also the first case that does not rely on radial-velocity observations, which are very challenging here because of the long orbital period ( $\sim 170$  yr) and the rapid rotation of the primary star. Instead, we have succeeded in deriving the masses using only astrometric observations. The key ingredients supplementing the visual measurements of the pair are the individual proper motions measured by *Gaia* for the two components, which, combined with the p.m. for the primary from the *Hipparcos* mission, provide the only constraint available on the mass ratio. We infer an orbit that is highly inclined and very eccentric ( $e = 0.915$ ), such that at closest approach the two stars come within about 3.7 au of each other.

A vexing problem in the use of visual observations for orbit computation is the assignment of realistic uncertainties, which are rarely reported for the historical measurements. While sensible, the weighting scheme adopted for those measurements in this work is by no means the only one possible. We note, for example that an earlier analysis we carried out leading up to the present one differed in three respects regarding the treatment of errors: 1) the observations were separated by date into three groups instead of four, giving lower weight to the speckle measurements than we do now; 2) constant errors in degrees were adopted for the position angles within each group, instead of constant errors in seconds of arc in the tangential direction, as we have done now to account for the error dependence on angular separation; and 3) no adjustment of the overall scale of the errors was made to balance the position angle and separation residuals, as done in the present work through the free parameters  $f_\rho$  and  $f_\theta$ . Reassuringly, despite these differences the mass estimates turn out to be very similar between the two procedures, suggesting little dependence on the details of how errors are assigned, at least in this particular case.

Our mass determinations along with those of the five previously known systems define an empirical MLR for the cluster in good agreement with current models of stellar evolution, given present uncertainties. We note, however, that several of the mass measurements—including our own—still have relative errors exceeding 10%, and

**Table 5**  
Dynamical Mass Determinations in the Hyades Cluster

Binary System	$M_A (M_\odot)$	$M_B (M_\odot)$	$M_V^A$ (mag)	$M_V^B$ (mag)	Source
$\theta^2$ Tau .....	$2.15 \pm 0.12$	$1.87 \pm 0.11$	$0.48 \pm 0.08$	$1.61 \pm 0.06$	Armstrong et al. (2006)
51 Tau .....	$1.80 \pm 0.13$	$1.46 \pm 0.18$	$2.14 \pm 0.10$	$3.75 \pm 0.17$	Torres et al. (1997a)
80 Tau .....	$1.63^{+0.30}_{-0.13}$	$1.11^{+0.21}_{-0.14}$	$2.283 \pm 0.012$	$4.664 \pm 0.017$	This work
70 Tau .....	$1.363 \pm 0.073$	$1.253 \pm 0.075$	$3.71 \pm 0.10$	$4.05 \pm 0.11$	Torres et al. (1997b)
$\theta^1$ Tau .....	...	$1.28 \pm 0.13$	...	$4.02 \pm 0.07$	Lebreton et al. (2001)
V818 Tau ....	$1.0591 \pm 0.0062$	$0.7605 \pm 0.0062$	$4.93 \pm 0.09$	$7.23 \pm 0.12$	Torres & Ribas (2002)

some of those determinations are now quite dated. New observations of higher quality may well be available in many cases. It seems likely that some of the masses could be improved considerably in both accuracy and precision with a self-consistent reanalysis of all available observations that avoids using partial results from earlier studies of these binaries. This would allow for a more stringent comparison with stellar evolution models than possible at this time.

We thank Robert Stefanik for bringing this system to our attention. We also thank Brian Mason for providing a listing of the measurements of 80 Tau from the Washington Double Star Catalog, and the anonymous referee for helpful comments. This work has been supported in part by grant AST-1509375 from the National Science Foundation. The research has made use of the SIMBAD and VizieR databases, operated at the CDS, Strasbourg, France, of NASA's Astrophysics Data System Abstract Service, and of the Washington Double Star Catalog maintained at the U.S. Naval Observatory. The work has also made use of data from the European Space Agency (ESA) mission *Gaia* (<https://www.cosmos.esa.int/gaia>), processed by the *Gaia* Data Processing and Analysis Consortium (DPAC, <https://www.cosmos.esa.int/web/gaia/dpac/consortium>). Funding for the DPAC has been provided by national institutions, in particular the institutions participating in the *Gaia* Multilateral Agreement.

## REFERENCES

- Abt, H. A., Sanwal, N. B., & Levy, S. G. 1980, *ApJS*, 43, 549  
 Armstrong, J. T., Mozurkewich, D., Hajian, A. R., et al. 2006, *AJ*, 131, 2643  
 Baize, P. 1980, *A&AS*, 39, 83  
 Balega, I. I., & Balega, Y. Y. 1988, *Soviet Astronomy Letters*, 14, 393  
 Brandt, T. D. 2018, *ApJS*, 239, 31  
 Brandt, T. D., Dupuy, T. J., & Bowler, B. P. 2019, arXiv e-prints, arXiv:1811.07285  
 Brandt, T. D., & Huang, C. X. 2015, *ApJ*, 807, 24  
 Burnham, S. W. 1906, *A General Catalogue of Double Stars within 121° of the North Pole*, (Washington: Carnegie Institution of Washington), p. 388  
 Chen, Y., Girardi, L., Bressan, A., et al. 2014, *MNRAS*, 444, 2525  
 Choi, J., Dotter, A., Conroy, C., et al. 2016, *ApJ*, 823, 102  
 Dupuy, T. J., Brandt, T. D., Kratter, K. M., et al. 2019, *ApJ*, 871, L4  
 Dutra-Ferreira, L., Pasquini, L., Smiljanic, R., et al. 2016, *A&A*, 585, A75  
 ESA, ed. 1997, *ESA Special Publication*, Vol. 1200, *The Hipparcos and Tycho Catalogues*  
 Evans, D. W., Riello, M., De Angeli, F., et al. 2018, *A&A*, 616, A4  
 Foreman-Mackey, D., Hogg, D. W., Lang, D., & Goodman, J. 2013, *PASP*, 125, 306  
 Foreman-Mackey, D. 2016, *The Journal of Open Source Software*, 24, <http://dx.doi.org/10.5281/zenodo.45906>  
 Gaia Collaboration, Brown, A. G. A., Vallenari, A., et al. 2018, *A&A*, 616, A1  
 Gelman, A., & Rubin, D. B. 1992, *Statistical Science*, 7, 457  
 Goodman, J., & Weare, J. 2010, *Commun. Appl. Math. Comput. Sci.*, 5, 65  
 Gregory, P. C. 2005, *ApJ*, 631, 1198  
 Heintz, W. D. 1981, *ApJS*, 46, 247  
 Høg, E., Fabricius, C., Makarov, V. V., et al. 2000, *A&A*, 355, L27  
 Izmailov, I. S. 2019, *Astronomy Letters*, 45, 30  
 Lampens, P., Torres, K., Frémat, Y., et al. 2009, *American Institute of Physics Conference Series*, 446  
 Lebreton, Y., Fernandes, J., & Lejeune, T. 2001, *A&A*, 374, 540  
 Martin, C., Mignard, F., Hartkopf, W. I., et al. 1998, *A&AS*, 133, 149  
 McClure, R. D. 1982, *ApJ*, 254, 606  
 Perryman, M. A. C., Brown, A. G. A., Lebreton, Y., et al. 1998, *A&A*, 331, 81  
 Peterson, D. M., & Solensky, R. 1988, *ApJ*, 333, 256  
 Peterson, D. M., Stefanik, R. P., & Latham, D. W. 1993, *AJ*, 105, 2260  
 Royer, F., Grenier, S., Baylac, M.-O., et al. 2002, *A&A*, 393, 897  
 Schiller, S. J., & Milone, E. F. 1987, *AJ*, 93, 1471  
 Söderhjelm, S. 1999, *A&A*, 341, 121  
 Struve, F. G. W. 1837, *Astronomische Nachrichten*, 14, 249  
 Tomkin, J., Pan, X., & McCarthy, J. K. 1995, *AJ*, 109, 780  
 Torres, G., & Ribas, I. 2002, *ApJ*, 567, 1140  
 Torres, G., Stefanik, R. P., & Latham, D. W. 1997a, *ApJ*, 474, 256  
 Torres, G., Stefanik, R. P., & Latham, D. W. 1997b, *ApJ*, 479, 268  
 Torres, G., Stefanik, R. P., & Latham, D. W. 1997c, *ApJ*, 485, 167  
 Torres, K. B. V., Lampens, P., Frémat, Y., et al. 2011, *A&A*, 525, A50  
 van Bueren, H. G. 1952, *Bull. Astron. Inst. Netherlands*, 11, 385  
 van Leeuwen, F. 2007, *Astrophysics and Space Science Library*